



Published in final edited form as:

Biomed Mater Eng. 2017 ; 28(2): 187–199. doi:10.3233/BME-171666.

An improved finite element modeling of the cerebrospinal fluid layer in the head impact analysis

John Z. Wu^a, Christopher S. Pan^{a,*}, Bryan M. Wimer^a, and Charles L. Rosen^b

^aNational Institute for Occupational Safety and Health, Morgantown, West Virginia, USA

^bDepartment of Neurosurgery, West Virginia University, Morgantown, West Virginia, USA

Abstract

The finite element (FE) method has been widely used to investigate the mechanism of traumatic brain injuries (TBIs), because it is technically difficult to quantify the responses of the brain tissues to the impact in experiments. One of technical challenges to build a FE model of a human head is the modeling of the cerebrospinal fluid (CSF) of the brain. In the current study, we propose to use membrane elements to construct the CSF layer. Using the proposed approach, we demonstrate that a head model can be built by using existing meshes available in commercial databases, without using any advanced meshing software tool, and with the sole use of native functions of the FE package Abaqus. The calculated time histories of the intracranial pressures at frontal, posterior fossa, parietal, and occipital positions agree well with the experimental data and the simulations in the literature, indicating that the physical effects of the CSF layer have been accounted for in the proposed modeling approach. The proposed modeling approach would be useful for bioengineers to solve practical problems.

Keywords

Biomechanics of impact; finite element analysis; head-brain impact; cerebrospinal fluid; traumatic brain injury

1. Introduction

Traumatic brain injury (TBI) occurs when a sudden trauma causes damage to the brain. During 2002–2006, approximately 1.7 million cases occurred in civilians annually [1]. A total of 7294 work-related TBI fatalities were identified during 2003–2008, which accounted for 22% of all occupational injury fatalities [2]. Among the leading causes of work-related TBI death, falls and contact with objects/equipment occupied 47% [2]. Generally, four approaches have been used to study the biomechanics of TBI: human cadaveric, animal,

*Corresponding author: Christopher S. Pan. cpan@cdc.gov.

Disclaimers

The findings and conclusions in this report are those of the authors and do not necessarily represent the views of the National Institute for Occupational Safety and Health. Mention of company names or products does not imply endorsement by the National Institute for Occupational Safety and Health.

Conflict of interest

The authors have no conflict of interest to report.

physical, and computer models. In the computer modeling approach, the finite element (FE) method or FE model is mainly utilized to study TBI. Because it is technically difficult to quantify the mechanical responses of the brain tissues to the impact in experiments, the FE method has been widely used to investigate the injury mechanism of TBI [3]. In order for the FE method to generate realistic simulations, the models must include real anatomic geometries, reliable material properties, and physiological boundary/loading conditions of the biological systems. Over the last three decades, much progress has been made in the development of human head FE models. The development of human head-brain modeling has progressed from early models with linear material properties and simplistic geometries (e.g., [4,5]) to the current sophisticated models including nonlinear and time-dependent material properties, realistic geometries, and detailed anatomical structures [6–8].

One of the technical challenges to build a FE model of a human head is the modeling of the cerebrospinal fluid (CSF) of the brain. The CSF is a body fluid that occupies the subarachnoid space around the brain and spinal cord and the ventricular system. Although the CSF layer has only a thickness of 1–5 mm [9–12], it is non-negligible in the modeling as it plays an important role in absorbing the dynamic energy transmitted to the brain during the impact [13]. In the previous FE models, the CSF has been constructed using solid elements. Using the traditional FE modeling method, it is necessary to have precise dimensions or geometries of the inside and outside surfaces to construct the CSF layer; this would require a fine mesh size in the region, due to the small thickness of the CSF layer, resulting in a substantial increase in the computational expenses. In many practical applications, such as the optimization design of construction helmets [14], equipment designers would use existing, generic head-brain meshes, which usually do not contain the geometries of the inside and outside surfaces of the CSF layer. Consequently, the CSF has been neglected in FE modeling for some applications [14].

In the studies of the mechanisms of TBIs, researchers are interested in the stress and strains in the brain, skull, skin, and other soft tissues in response to the impact. Researchers are also interested in the role of CSF in the transmission of the dynamic loading, however, in many cases, precise surface geometries of the CSF layer are not available. In this scenario, it is possible to model the CSF layer using structural elements to simplify the FE modeling. Our hypothesis is that the CSF can be simulated using membrane elements, in which the shear stress and stress/strain gradients across the thickness are neglected. The purpose of this study is to develop a practical FE modeling tool that would be suitable for practical use in ergonomic or bioengineering design. Our FE model will be constructed using the commercially available FE software Abaqus and using the meshes available in an existing, generic database and, meanwhile, it will contain all essential anatomical structures of a human head, which includes the skin, scalp, skull, cerebrospinal fluid (CSF), brain (cerebrum/cerebellum/pons/peduncles), medulla, spinal cord, cervical vertebrae, and discs.

2. Method

2.1. Finite element model

The FE model contains a head-brain-neck complex and it is constructed by using surface scans, which were obtained from a commercial data base (Materialise, Leuven, Belgium).

<http://biomedical.materialise.com>). The model was constructed by using three surface scans: the external skin (Fig. 1(A)), skull (Fig. 1(B)), and brain (Fig. 1(C)). The model dimensions represent approximately the 50th percentile of Caucasian males.

The model consists of three solid, volumetric regions (i.e., external soft tissues, skull, and brain) (Fig. 2(A), (B), and (D)) and one membrane region (i.e., CSF) (Fig. 2(C)). The volumetric region of the external soft tissues (Fig. 2(A)) was generated from the external skin scan (Fig. 1(A)) by excluding the volume of the skull (Fig. 1(B)). The volumetric region of the skull (Fig. 2(B)) was generated from the skull (Fig. 1(B)) by excluding the volume of the brain (Fig. 1(C)). The external brain scan (Fig. 1(C)) was utilized to generate both the volumetric region of the brain (Fig. 2(D)) and the CSF membrane region (Fig. 2(C)). The entire FE model was constructed by using a commercially available software ABAQUS (version 6.9, Dassault Systems, Waltham, Massachusetts, USA); no other advanced meshing software was needed to generate the current FE model.

The volumetric region of the external soft tissues (Fig. 2(A)) was further divided into the scalp and skin tissues. The volumetric region of the skull (Fig. 2(B)) was further divided into the skull bone, cervical vertebrae (C1, C2, and C3), and discs; the discs contained both annulus fibrosus and nucleus pulposus. The volumetric region of the brain (Fig. 2(C)) was further divided into three parts: brain (cerebrum/cerebellum/pons/peduncles), brain lobe or medulla (a part of brainstem), and spinal cord. The CSF layer (Fig. 2(C)) was considered to cover the entire external surface of the brain, brainstem, and the spinal cord (Fig. 2(D)). The entire head-brain-neck complex is illustrated in (Fig. 3(A)).

The CSF (Fig. 2(C)) was constructed using membrane elements (element: M3D8), whereas all other components (Fig. 2(A), (B), and (D)) were constructed using three-dimensional (3D) continuous solid elements (elements: C3D4 and C3D10). Within each of these anatomical components (i.e., brain, medulla, CSF, spinal cord, and discs), the material was considered homogeneous. The connections between the tissues were assumed to be perfect bond, without relative sliding during deformation. The internal surface of the CSF layer was constrained to the external surface of the brain/spinal cord complex (Fig. 2(D)); the external surface of the CSF was constrained to the internal surface of the skull/vertebra/disc complex (Fig. 2(B)). Although the thickness of the CSF was not visually seen in the model, its physical functionality was included in the modeling.

2.2. Material properties

The scalp, skull bone, cervical discs, and vertebral bone were considered to be linearly elastic. The elastic modulus and Poisson's ratio of the scalp ($E = 16.7$ MPa and $\nu = 0.42$) were assumed based on the experimental data by [15] and the viscous deformation was neglected. The material properties of the cervical discs ($E = 4.8$ MPa and $\nu = 0.22$) were based on the test data by [16]; the effects of the interstitial fluid were neglected. The same elastic material properties were applied to the skull and vertebral bone ($E = 6.0$ GPa and $\nu = 0.19$) [17]. The CSF had a thickness of 1.3 mm and was considered as an elastic and incompressible medium with a small shear modulus [6] ($E_1 = E_2 = 150$ kPa, $\nu_{12} = 0.4999$, and $G_{12} = 0.01$ kPa).

The skin, brain, medulla, and spinal cord were considered to be hyperelastic and viscoelastic. The finite deformation formulation was used in describing the constitutive models due to large tissue deformations. The formulations of finite deformation algorithm in the finite element analysis have been described in detail in the literature [18,19]. The hyperelastic properties of the skin, brain, brain stem, and spinal cord tissues were modeled using a two term Mooney–Rivlin equation, which is governed by a strain energy potential:

$$U = C_{10}(\bar{I}_1 - 3) + C_{11}(\bar{I}_1 - 3)(\bar{I}_2 - 3) + \frac{1}{D_1}(J - 1)^2 \quad (1)$$

where \bar{I}_1 , \bar{I}_2 , and J is the first and second deviatoric strain invariants, and the volumetric ratio, respectively; C_{10} , C_{11} , and D_1 are the material parameters.

Neglecting the volumetric viscoelastic deformation, the shear viscoelastic properties of the tissues were determined by two-term Prony series:

$$g(t) = 1 - \sum_{i=1}^2 g_i(1 - e^{-\frac{t}{\tau_i}}) \quad (2)$$

where g_i and τ_i ($i = 1, 2$) are shear and relaxation time parameters, respectively.

The nonlinearly elastic properties of the skin ($C_{10} = 9.4$ kPa, $C_{11} = 82$ kPa and $D_1 = 0.001$ kPa⁻¹) were determined by using the in vivo test data of human skin by [20] and [21]; the viscoelastic properties of the skin ($g_1 = 0.295$, $g_2 = 0.349$, $\tau_1 = 0.372$ s, and $\tau_2 = 5.593$ s) were determined based on [22]. The viscous properties ($g_1 = 0.8973$, $g_2 = 0.0741$, $\tau_1 = 0.0047$ s, and $\tau_2 = 1.4538$ s) and the nonlinear elastic parameters ($C_{10} = 0.75$ kPa and $D_1 = 0.001$ kPa⁻¹) of the medulla were determined based on the data by [23]. The nonlinear elastic ($C_{10} = 14.8$ kPa and $D_1 = 0.001$ kPa⁻¹) and viscoelastic properties ($g_1 = 0.5200$, $g_2 = 0.3057$, $\tau_1 = 0.0264$ s, and $\tau_2 = 0.011$ s) of the spinal cord were determined based on the data by [24] and [25].

The FE model was tested using a linear elastic and a hyperelastic material model for the brain tissues. The linear viscoelastic properties ($E = 22.8$ kPa, $\nu = 0.49992$, $g_1 = 0.815$, and $\tau_1 = 0.00143$ s) of the brain tissues were based on the test data by [8]. The parameters of the hyperelastic brain model ($C_{01} = 3.8$ kPa, $C_{11} = 7.6$ kPa, linear and $D_1 = 4.21 \cdot 10^{-5}$ kPa⁻¹) were estimated using the parameters of the elastic model by

$$C_{01} = \frac{E}{4(1 + \nu)}, \quad C_{11} = 2C_{01}, \quad D_1 = \frac{6(1 - 2\nu)}{E}. \quad (3)$$

Under uniaxial compression/tension, the stress-strain relation of the hyperelastic model is compared with that of the linearly elastic model in Fig. 4. The stress-strain curve for the

hyperelastic model tends to convert to that of the linearly elastic model for infinitesimal strain.

All material parameters of the hard and soft tissues used in the current model are listed in Table 1. The entire model contains 45,771 elements, 37,776 nodes, and 292,115 degrees of freedom (DOFs), and has a mass of 4.735 kg.

2.3. Procedures of the numerical tests

The set-up of the numerical impact test was constructed to mimic the cadaveric tests by [26], as illustrated in Fig. 3(B). The head-brain model was tilted forward, making the Frankfort anatomical plane incline by 45° to the horizontal plane. A cylindrical object impacted at the forehead in the mid-sagittal plane. The impacting object had a diameter of 50 mm and a height of 30 mm; the object was assumed to have a negligible mass compared with the head model. The impact force, as measured in the experiment [26], was applied uniformly at the back of the cylindrical impact object (Fig. 3(B)). The simulations were conducted in a force controlled manner; no boundary conditions were applied on the model. In the impact tests by [26], the intracranial pressures were measured at the frontal, parietal, occipital, and posterior fossa locations, as illustrated in (Fig. 5); they will be used for the validation of the current model. The head accelerations and the pressures in the brain tissues at four locations (Fig. 5) calculated using the proposed model will be compared with the experimental data by [26] and the simulation results by [27] and [8].

3. Results

Simulations were performed by using both linearly elastic and hyperelastic models for the brain tissues (Table 1). We found that the results obtained by using the linear brain model are identical to those obtained by using hyperelastic brain model, as expected. Consequently, we only show the simulation results obtained by using the hyperelastic brain models.

The predicted responses of the head and brain during impact were compared with those measured in experiments by [26] (Test #37 in [26]) in Fig. 6. Figure 6(A) shows the time-history of the impact force measured in the experiment [26], which was applied as input in the current FE simulations. For the purpose of verification, the calculated contact force between the impact object and the head was also compared with the experimental data (Fig. 6(A)) and they agree well. The calculated acceleration magnitudes at the skull, skin, and medulla are compared with the corresponding experimental data, as shown in Fig. 6(B). The acceleration shown in the plots was considered as the vectorial sum of the acceleration components in three orthogonal directions. It is seen that the calculated acceleration at the skin is approximately consistent with that obtained in the experiment [26], while the acceleration at the skull and medulla is approximately 20% lower and 16% higher, respectively, than the experimental data.

The calculated intracranial pressures are compared with the FE simulations in the literature [8,27] and the experimental data [26] at the frontal, posterior fossa, parietal, and occipital positions, as shown in Fig. 7(A), 7(B), 7(C), and 7(D), respectively. In the FE modeling, the mechanical pressures in the brain tissues were considered as the intracranial pressures.

For $t = 6$ ms, when the intracranial pressures reach the maximums (Fig. 7), the distributions of the intracranial pressures and accelerations in the brain tissues are shown in Fig. 8(A) and (B), respectively. The left column of the plots shows the distributions on the surface of the brain, while the right column of the plots shows the distributions in the central cross-section of the brain model. The maximal and the minimal values of the intracranial pressures are found at the surface of the brain (Fig. 8(A)), while the maximal acceleration magnitude is found at the center of medulla region (Fig. 8(B), right).

4. Discussion and conclusion

The CSF plays an important role in absorbing the dynamic energy transmitted to the brain during the impact. The modeling of the CSF layer in a human head FE model is a technical challenge for bio-engineers. In the current study, we proposed to use membrane elements to construct the CSF layer. The major advantage of the use of the membrane elements over the traditional modeling method is that the model can be built without the precise scans of the internal and external surfaces of the CSF layer, and that the model can be constructed using relatively coarser meshes for the CSF layer, reducing computational expenses. Using the proposed approach, we built a FE model of human head-brain complex by using existing meshes available in commercial database (Materialise, Leuven, Belgium), without using any advanced meshing software tool, and with the sole use of the native functions of the FE package Abaqus.

Traditionally, CSF has been modeled using 3D solid elements [6,8]. To construct a solid 3D model will necessitate precise scans of both the inside and outside surfaces of the CSF. In addition, because of the small thickness of the CSF, the mesh density has to be much higher using 3D solid elements than when using the membrane elements. Application of the membrane elements made it possible to greatly reduce the model size (in term of DOF). The proposed method would be useful for ergonomic designers or biomedical engineers, who have to develop their FE models based on scans from generic, commercial or public databases, which usually do not contain detailed geometries of the subarachnoid space around the brain.

The predicted time histories of the intracranial pressures at frontal, posterior fossa, parietal, and occipital positions using our model agree well with the experimental data [26] and simulations [8,27] in the literature, indicating that the physical effects of the CSF layer have been accounted for in the proposed modeling approach.

Our simulation results indicated that the maximal acceleration magnitude did not appear on the surface of the brain tissues, but in the core of the medulla region of the brain, although the maximal/minimal pressures were found on the surface of the brain (Fig. 8). This finding is significant because the brain acceleration has been traditionally used as the injury criteria in the ergonomic design. For example, the head injury criteria (HIC) [28,29], which is widely accepted in the research and development in the automobile industries, is based on the time histories of the head accelerations obtained in the experiments. However, the accelerations are measured on the skin surface in the conventional engineering analysis. Our results indicated that the accelerations on the skin of the head would be approximately 12%

lower than the maximal accelerations, which appear in the medulla region. Our findings are also consistent with the clinical observations that the medulla appeared to be one of the most vulnerable parts during a TBI [30].

A further advantage of the proposed approach is the correct representation of the material property of the CSF. Because the CSF is a fluid, it should be nearly incompressible and has a small shear modulus. In the membrane elements of the CSF layer, as in the proposed model, the shear modulus is excluded. In the FE model by [8], the CSF is considered as a liquid, which is completely incompressible and has a zero shear modulus. However, in early FE models, the CSF is considered as an elastic, isotropic medium, in which the CSF material could be nearly incompressible, but will have a considerable shear modulus. The FE simulations by [27] indicated that the shear modulus of the CSF have a non-negligible effects on the intracranial pressures. However, when the head-brain is subjected to a linear acceleration, the effect of the shear modulus on the intracranial pressures is small [31].

In summary, we proposed an approach to model the CSF layer in a human head FE model. Using the proposed approach, we demonstrated that a head model can be built by using existing meshes available in commercial databases, without using any advanced meshing software tool, and with the sole use of native functions of the FE package Abaqus. The proposed modeling approach would be useful for bioengineers or designers to solve practical problems.

Acknowledgments

Funding

This study was supported by a research grant of CDC foundation. We want to express our gratitude to Turner Construction Company, Liberty Mutual Insurance, Zurich Insurance Group, and ACE Group for their generous donations to that research grant via CDC Foundation.

References

- [1]. Faul M, Xu L, Wald MM and Coronado VG, Traumatic brain injury in the united states: Emergency department visits, hospitalizations and deaths 2002–2006, Technical Report, Atlanta (GA), Centers for Disease Control and Prevention, 2010.
- [2]. Tiesman HM, Konda S and Bell JL, The epidemiology of fatal occupational traumatic brain injury in the U.S., *Am J Prev Med* 41(1) (2011), 61–67. doi:10.1016/j.amepre.2011.03.007. [PubMed: 21665064]
- [3]. Voo K, Kumaresan S, Pintar FA, Yoganandan N and Sances A, Jr., Finite-element models of the human head, *Med Biol Eng Comput* 34(5) (1996), 375–381. doi:10.1007/BF02520009. [PubMed: 8945864]
- [4]. Hardy CH and Marcal PV, Elastic analysis of a skull, *ASME J. Appl. Mech* 40 (1973), 838–842. doi:10.1115/1.3423172.
- [5]. Kenner VH and Goldsmith W, Dynamic loading of a fluid-filled spherical shell, *Int J Mech Sci* 14(9) (1972), 557–568. doi:10.1016/0020-7403(72)90056-2.
- [6]. Willinger R, Kang HS and Diaw B, Three-dimensional human head finite-element model validation against two experimental impacts, *Ann Biomed Eng* 27(3) (1999), 403–410. doi: 10.1114/1.165. [PubMed: 10374732]
- [7]. Kleiven S and Hardy WN, Correlation of an FE model of the human head with local brain motion – consequences for injury prediction, *Stapp Car Crash J* 46 (2002), 123–144. [PubMed: 17096222]

- [8]. Yan W and Pangestu OD, A modified human head model for the study of impact head injury, *Comput Methods Biomech Biomed Engin* 14(12) (2011), 1049–1057. doi: 10.1080/10255842.2010.506435. [PubMed: 21264785]
- [9]. Jernigan TL, Zatz LM, Ahumada AJ, Jr., Pfefferbaum A, Tinklenberg JR and Moses JA, Jr., Ct measures of cerebrospinal fluid volume in alcoholics and normal volunteers, *Psychiatry Res* 7(1) (1982), 9–17. doi:10.1016/0165-1781(82)90048-8. [PubMed: 6957902]
- [10]. Kohn MI, Tanna NK, Herman GT, Resnick SM, Mozley PD, Gur RE, Alavi A, Zimmerman RA and Gur RC, Analysis of brain and cerebrospinal fluid volumes with mr imaging. Part i. Methods, reliability, and validation, *Radiology* 178(1) (1991), 115–122. doi:10.1148/radiology.178.1.1984289. [PubMed: 1984289]
- [11]. Ryan J, Artero S, Carriere I, Scali J, Maller JJ, Meslin C, Ritchie K, Scarabin PY and Ancelin ML, Brain volumes in late life: Gender, hormone treatment, and estrogen receptor variants, *Neurobiol Aging* 35(3) (2014), 645–654. doi:10.1016/j.neurobiolaging.2013.09.026. [PubMed: 24269019]
- [12]. Mandell JG, Kulkarni AV, Warf BC and Schiff SJ, Volumetric brain analysis in neurosurgery: Part 2. Brain and csf volumes discriminate neurocognitive outcomes in hydrocephalus, *J Neurosurg Pediatr* 15(2) (2015), 125–132. doi:10.3171/2014.9.PEDS12427. [PubMed: 25431901]
- [13]. Baeck K, Goffin J and Sloten JV, The use of different csf representations in a numerical head model and their effect on the results of fe head impact analyses, in: 8th European LS-DYNA Users Conference, Strasbourg, 2011.
- [14]. Long J, Yang J, Lei Z and Liang D, Simulation-based assessment for construction helmets, *Comput Methods Biomech Biomed Engin* 18(1) (2015), 24–37. doi: 10.1080/10255842.2013.774382. [PubMed: 23495784]
- [15]. Galford JE and McElhaney JH, A viscoelastic study of scalp, brain, and dura, *J Biomech* 3(2) (1970), 211–221. doi:10.1016/0021-9290(70)90007-2. [PubMed: 5521539]
- [16]. Schmidt H, Haussler K, Wilke HJ and Wolfram U, Structural behavior of human lumbar intervertebral disc under direct shear, *J Appl Biomater Funct Mater* 13(1) (2015), 66–71. [PubMed: 24744233]
- [17]. Yamada H and Evans FG, *Strength of Biological Materials*, Williams and Wilkins, 1970.
- [18]. Abaqus theoretical manual, V 6.9. Dassault Systemes Simulia Corp, Providence, RI, USA, 2009.
- [19]. De Borst R, Crisfield MA, Remmers JJC and Verhoosel CV, *Nonlinear Finite Element Analysis of Solids and Structures*, 2nd edn, John Wiley & Sons, Ltd., West Sussex, UK, 2012 ISBN-13:978-0470666449, ISBN-10:0470666447.
- [20]. Hendriks FM, Brokken D, van Eemeren JT, Oomens CW, Baaijens FP and Horsten JB, A numerical-experimental method to characterize the non-linear mechanical behaviour of human skin, *Skin Res Technol* 9(3) (2003), 274–283. doi:10.1034/j.1600-0846.2003.00019.x. [PubMed: 12877691]
- [21]. Hendriks FM, Brokken D, Oomens CW and Baaijens FP, Influence of hydration and experimental length scale on the mechanical response of human skin in vivo, using optical coherence tomography, *Skin Res Technol* 10(4) (2004), 231–241. doi:10.1111/j.1600-0846.2004.00077.x. [PubMed: 15479446]
- [22]. Wu JZ, Dong RG, Smutz WP and Schopper AW, Nonlinear and viscoelastic characteristics of skin under compression: Experiment and analysis, *Biomed Mater Eng* 13(4) (2003), 373–385. [PubMed: 14646052]
- [23]. Arbogast KB and Margulies SS, Material characterization of the brainstem from oscillatory shear tests, *J Biomech* 31(9) (1998), 801–807. doi:10.1016/S0021-9290(98)00068-2. [PubMed: 9802780]
- [24]. Bilston LE and Thibault LE, The mechanical properties of the human cervical spinal cord in vitro, *Ann Biomed Eng* 24 (1996), 67–74. doi:10.1007/BF02770996. [PubMed: 8669719]
- [25]. Mazuchowski EL and Thibault LE, Biomechanical properties of the human spinal cord and pia mater, 6 25–29, 2003.
- [26]. Nahum AM, Smith R and Ward CC, Intra cranial pressure dynamics during head impact, in: *Proceedings of the 21st Stapp Car Crash Conference*, 1977, pp. 339–366.

- [27]. Horgan TJ and Gilchrist MD, The creation of three-dimensional finite element models for simulating head impact biomechanics, *International Journal of Crashworthiness* 8(4) (2003), 353–366. doi:10.1533/ijcr.2003.0243.
- [28]. Eppinger RH, A prospective view of head injury research, in: *Traumatic Brain Injury – Bioscience and Mechanics*, Bandak FA, Eppinger RH and Ommaya AK, eds, Mary Liebert, Inc., Larchmont, NY, 1996, pp. 39–45, chapter 5. ISBN:913113-73-5.
- [29]. Patel A and Goswami T, Comparison of intracranial pressure by lateral and frontal impacts – validation of computational model, 2012.
- [30]. Zivkovic V, Nikolic S, Strajina V, Djonc D, Babic D and Djuric M, Pontomedullary lacerations in pedestrians: An autopsy study, *Med Sci Law* 52(2) (2012), 107–111. doi:10.1258/msl.2011.011032. [PubMed: 22422786]
- [31]. Zhao W, Ruan S and Ji S, Brain pressure responses in translational head impact: A dimensional analysis and a further computational study, *Biomech Model Mechanobiol* 14(4) (2015), 753–766. doi:10.1007/s10237-014-0634-0. [PubMed: 25412925]

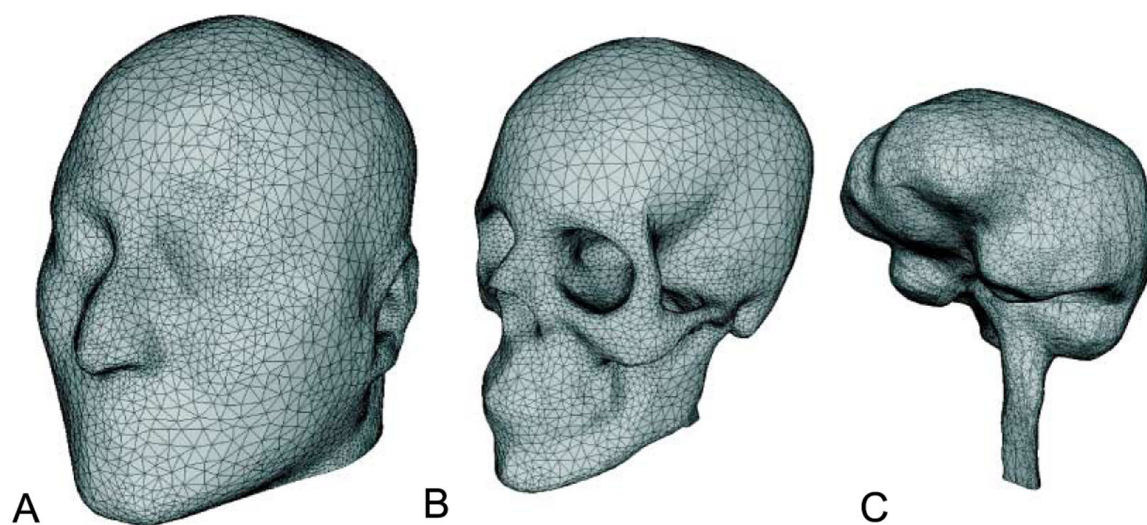


Fig. 1.
The original scans used to construct the proposed FE model. (A) Skin, (B) Skull, (C) Brain.

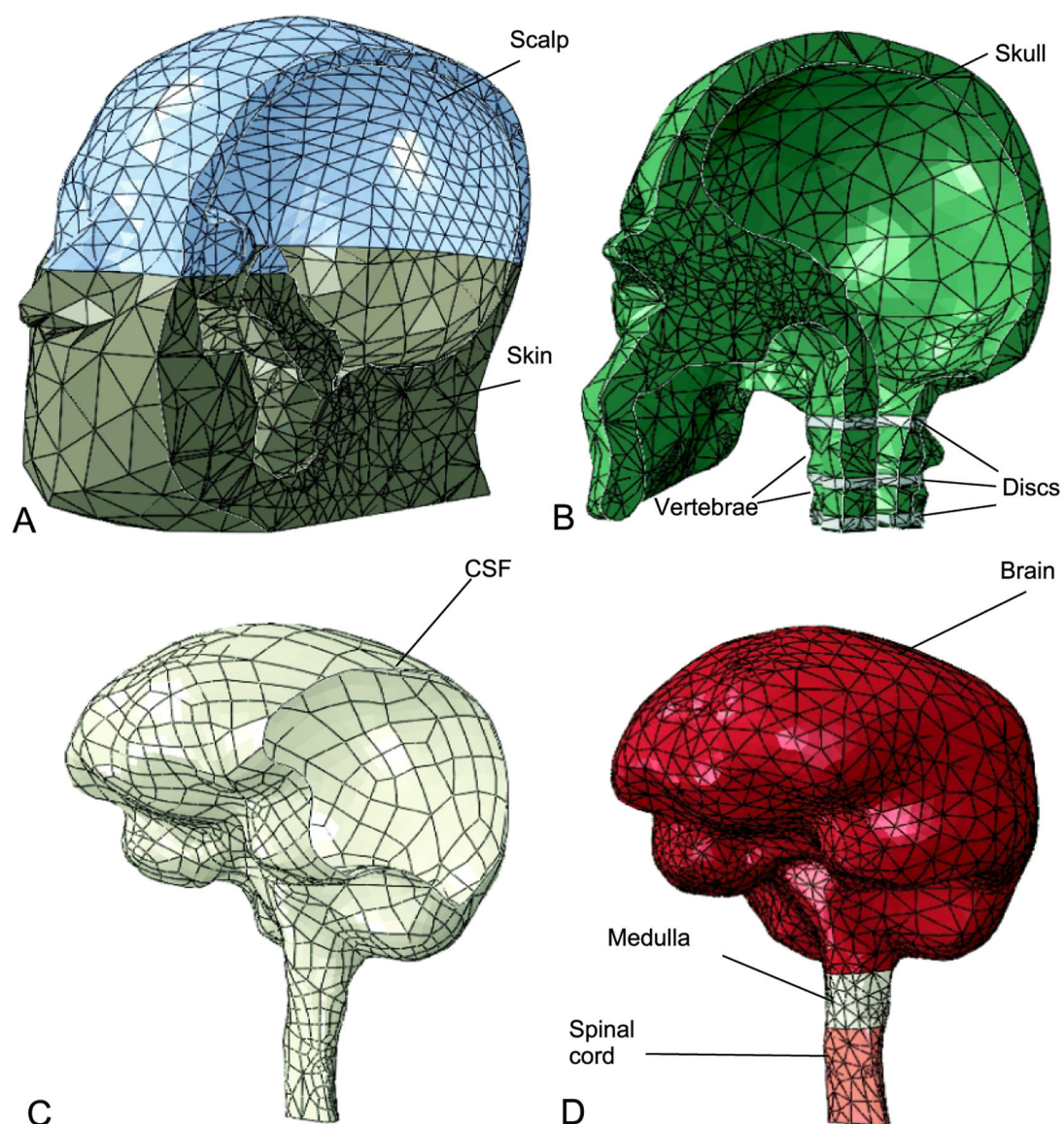


Fig. 2. Components of the FE model. (A) Scalp and skin tissues. (B) Skull, vertebrae, and discs. (C) Cerebrospinal fluid (CSF) layer. (D) Brain, medulla, and spinal cord.

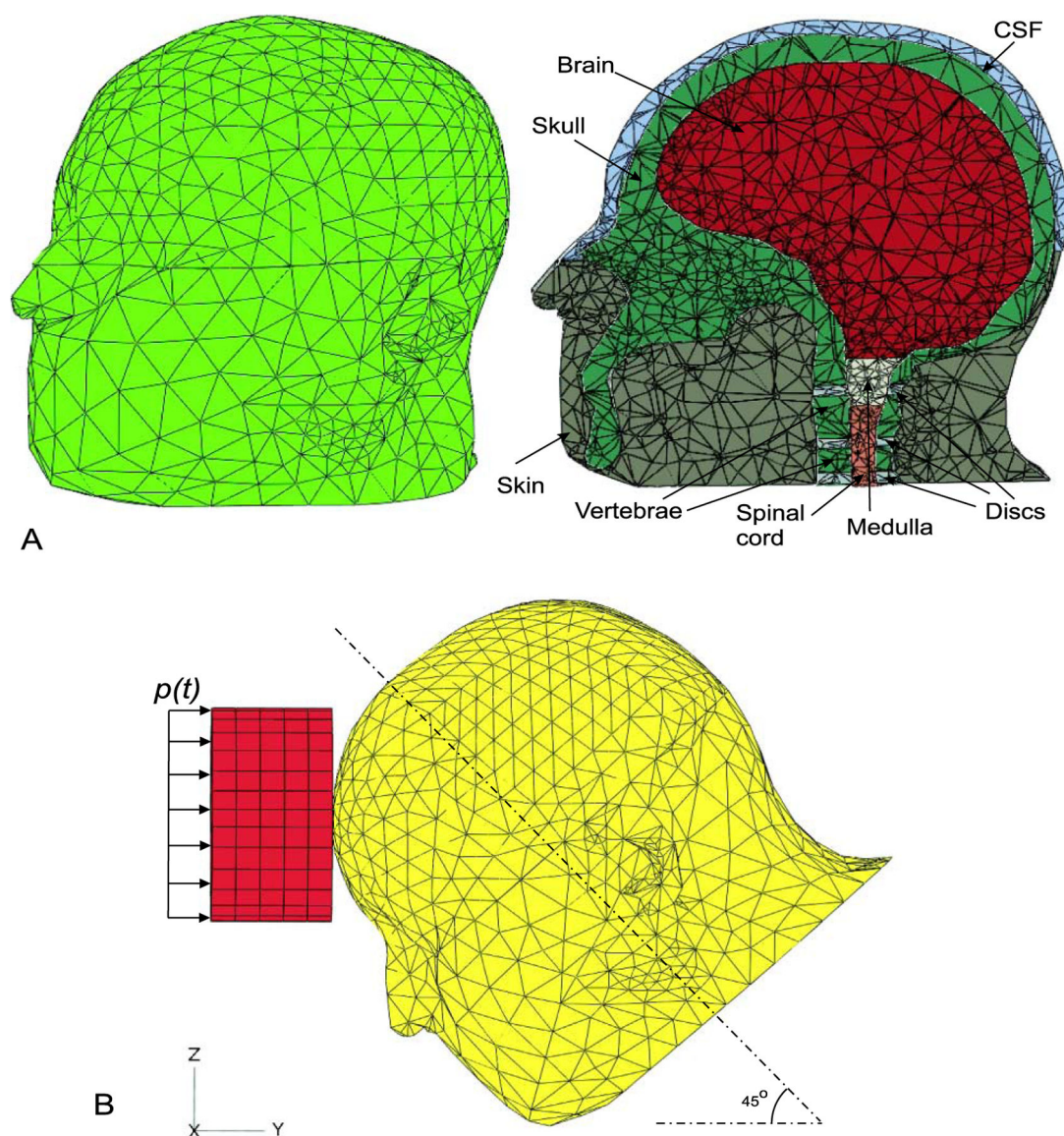


Fig. 3. FE modeling of the human head-brain and the numerical test. (A) FE model of the human head. Left: external view. Right: cross-sectional view. (B) Set-up of the numerical test. A distributed load was applied on the back of the cylindrical impact pad.

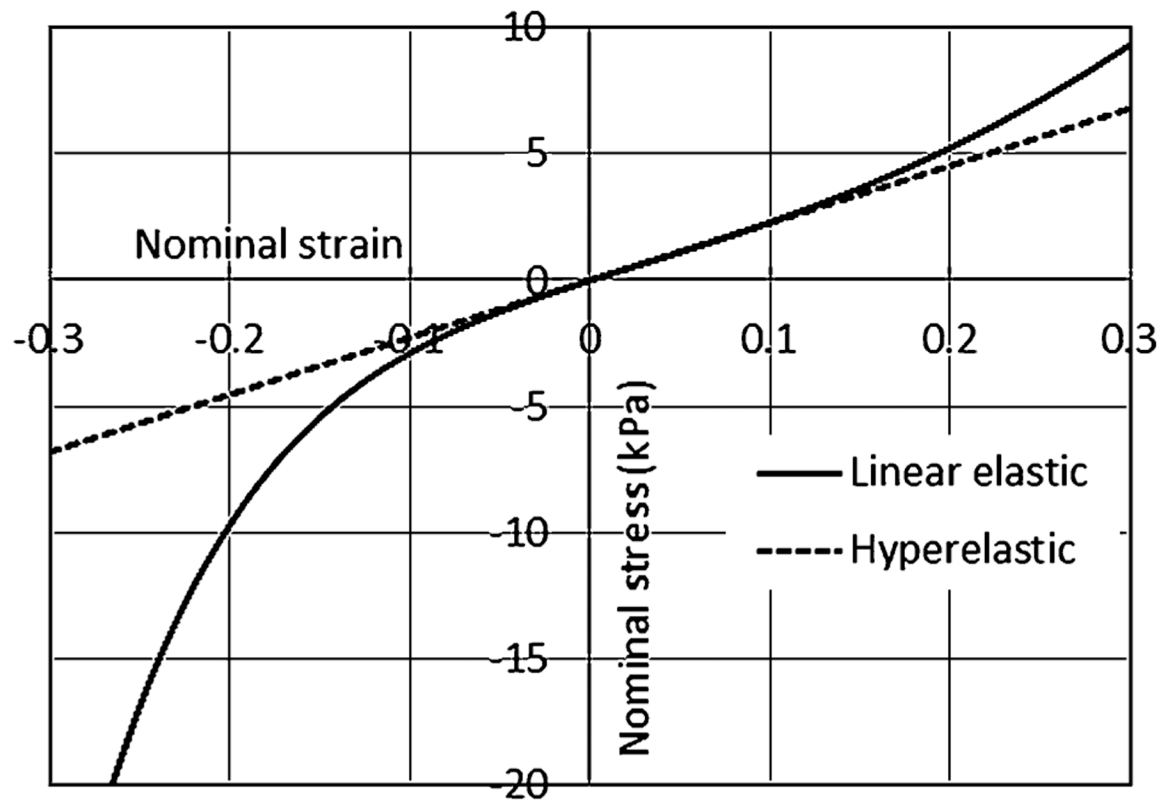


Fig. 4.

The comparison of the stress-strain relationship of the linear elastic with that of the hyperelastic brain models under uniaxial compress/tension. The parameters of the linear elastic model are adopted from Yan and Pangestu [8].

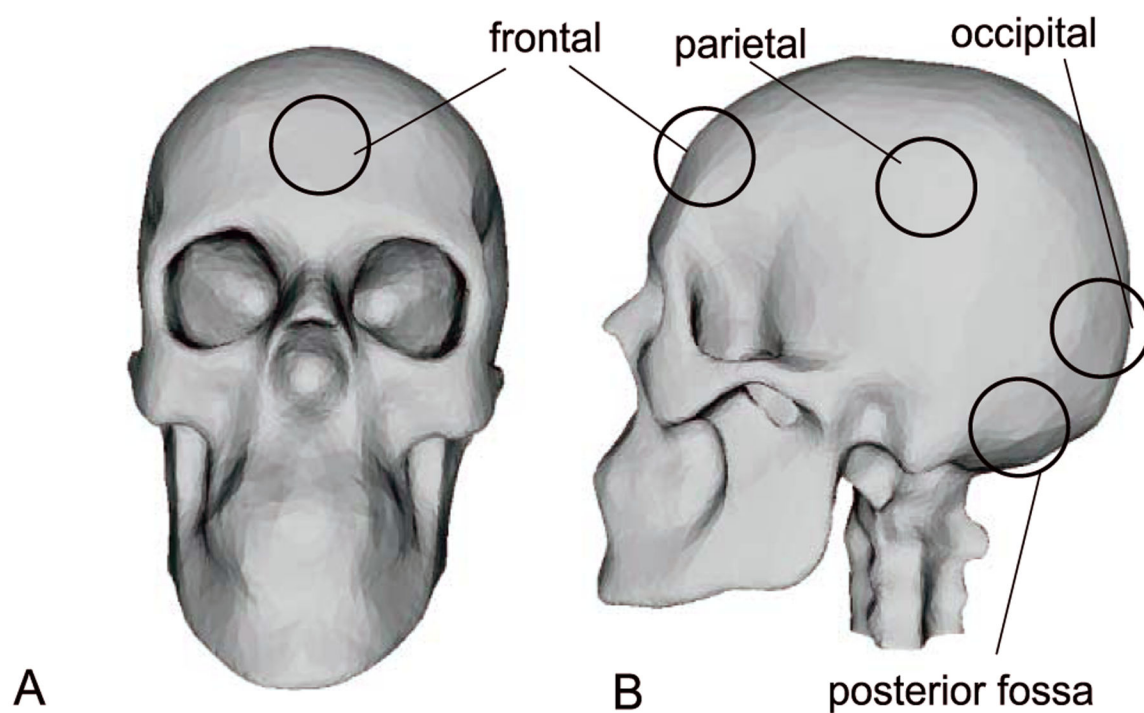
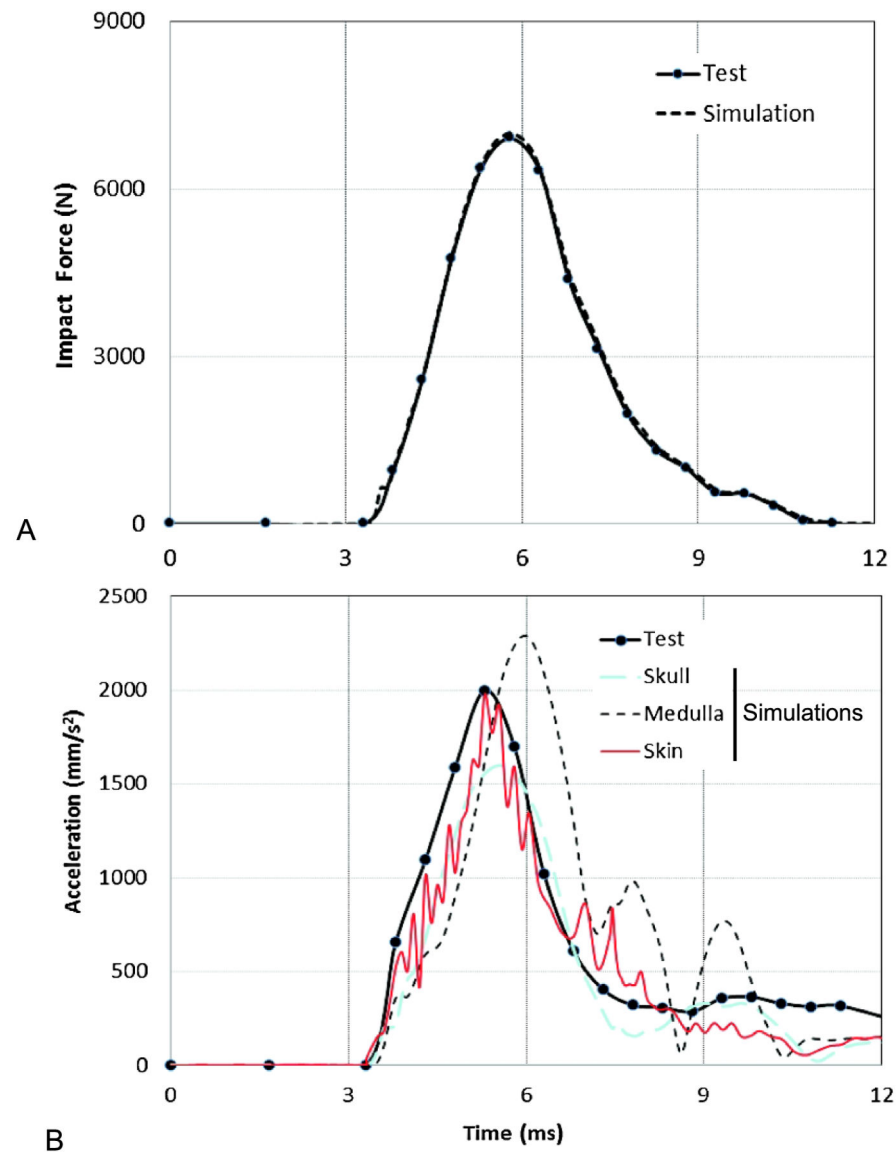
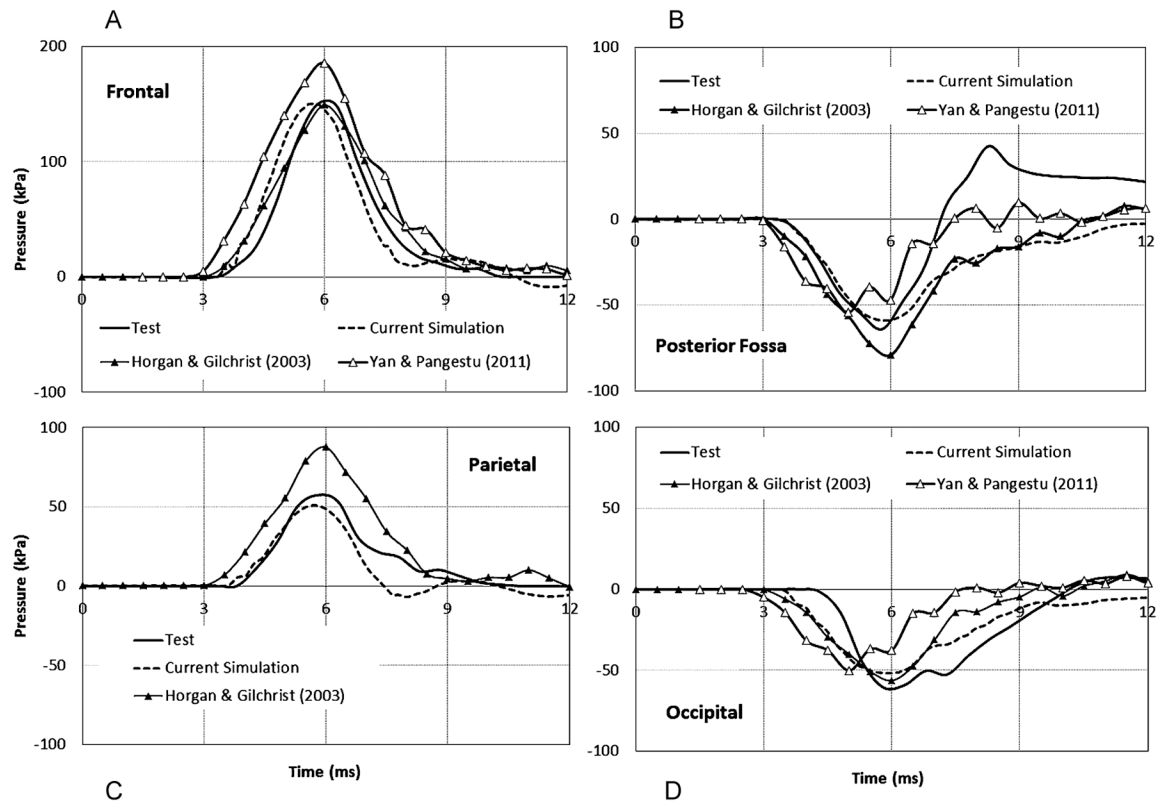


Fig. 5. Illustrate of the definition of the anatomical locations on a skull. The brain pressures at the frontal, posterior fossa, parietal, and occipital positions were measured in the experiment by (Nahum et al. [26]) and they will be used in the model validation.

**Fig. 6.**

The comparison of the impact force and head acceleration calculated using the proposed FE model with those measured in the experiment. (A) Impact force. (B) Acceleration magnitude. Impact force measured in the test (Nahum et al. [26]) was applied as the input for the current FE model. The acceleration magnitudes calculated at the skull, medulla, and skin using the proposed FE model are compared with the experimental data by Nahum et al. [26].

**Fig. 7.**

The brain pressures at the frontal (A), posterior fossa (B), parietal (C), and occipital (D) locations. The brain pressures at four locations calculated using the proposed FE model are compared with the simulations by Horgan and Gilchrist [27], by Yan and Pangestu [8], and the experimental data by Nahum et al. [26].

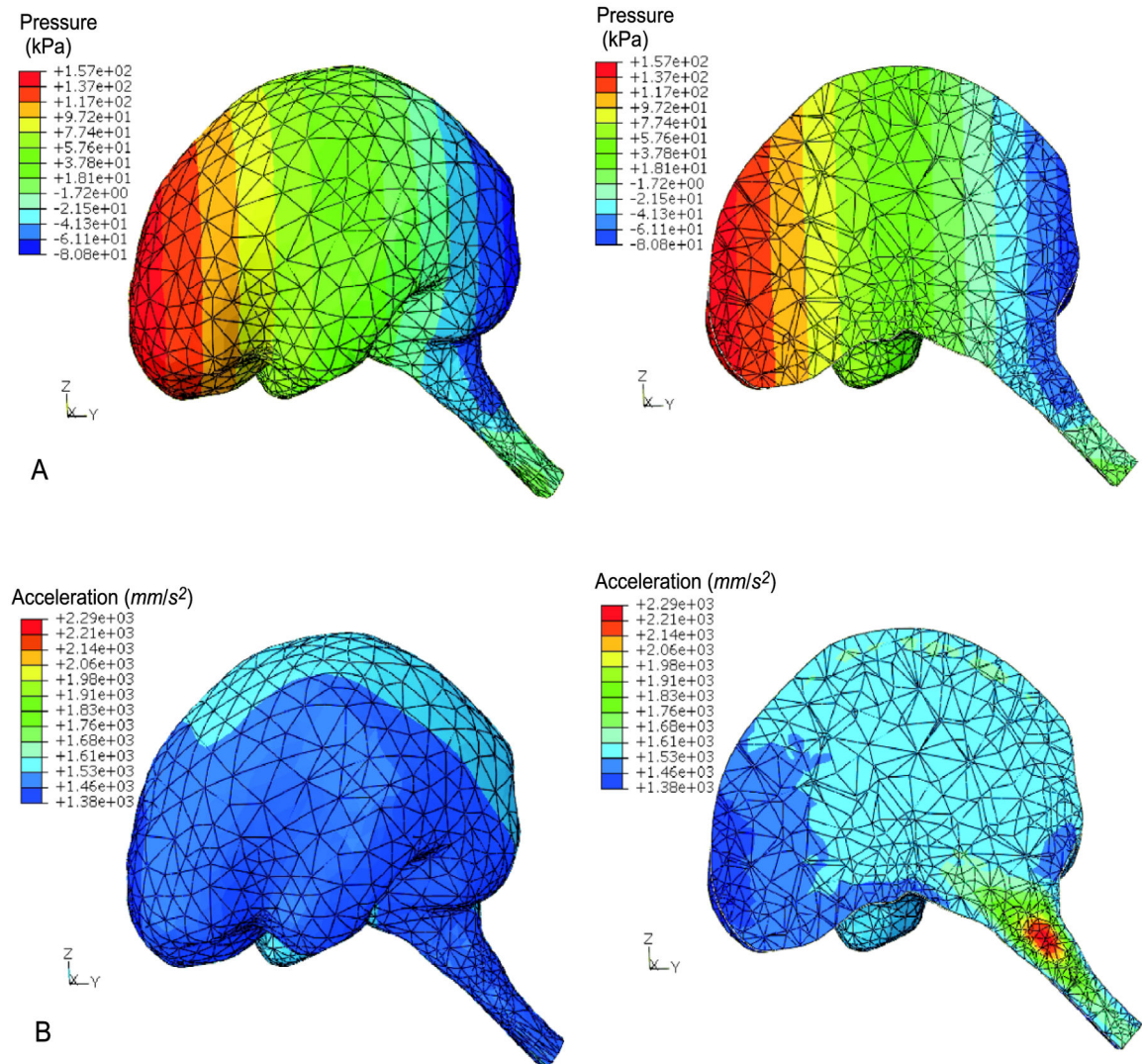


Fig. 8.

The distributions of the pressure and acceleration magnitude in the brain at $t = 6$ ms, when the impact force reached the maximum. (A) Brain pressure. (B) Acceleration magnitude. The left and right column of the plots show the distributions on the surface and at the central cross-section of the model, respectively.

Table 1

The material parameters of the hard and soft tissues used in the FE modeling

Materials (References)	Specific density	Elastic properties E, G, C_{10}, C_{11} (kPa) D_1 (kPa ⁻¹); ν (-)	Viscous properties (β)	Damping (s)
Brain		<i>Linear model:</i>		
(Yan and Pangestu [8])	1.05	$E = 22.8, \nu = 0.49992$	$g_1 = 0.815, \tau_1 = 0.00143$	0.001
		<i>Nonlinear model:</i>		
	1.05	$C_{10} = 3.80, C_{11} = 7.60,$ $D_1 = 4.21 \cdot 10^{-5}$	$g_1 = 0.815, \tau_1 = 0.00143$	0.001
Medulla	1.05	$C_{10} = 0.75, D_1 = 0.001$	$g_1 = 0.8973, g_2 = 0.0741,$ $\tau_1 = 0.0047, \tau_2 = 1.4538$	0.001
(Arbogast and Margulies [23])				
Spinal cord	1.05	$C_{10} = 14.8, D_1 = 0.001$	$g_1 = 0.52, g_2 = 0.3057,$ $\tau_1 = 0.0264, \tau_2 = 0.011$	0.001
(Mazuchowski and Thibault [25])				
(Bilston and Thibault [24])				
Skin	1.01	$C_{10} = 9.4, C_{11} = 82,$ $D_1 = 0.01$	$g_1 = 0.295, g_2 = 0.349,$ $\tau_1 = 0.373, \tau_2 = 5.592$	0.01
(Hendriks et al. [20] and [21])				
(Wu et al. [22])				
Scalp	1.01	$E = 16.7 \cdot 10^3, \nu = 0.42$		0.001
(Galford and McElhaney [15])				
Discs	1.01	$E = 4.8 \cdot 10^3, \nu = 0.22$		0.001
(Schmidt et al. [16])				
Bone (skull/vertebrae/spongy)	1.80	$E = 6.0 \cdot 10^6, \nu = 0.19$		0.001
(Yamada and Evans [17])				
CSF	1.0	$E_1 = E_2 = 150, \nu_{12} = 0.5,$ $G_{12} = G_{13} = G_{23} = 0.01$		0.001
(Yan and Pangestu [8])				